Int. J. Electrochem. Sci., 10 **(2015)** 9028 - 9041

International Journal of
ELECTROCHEMICAL
SCIENCE
www.electrochemsci.org

Inhibition Action and Adsorption Behavior of Green Inhibitor Sodium Carboxymethyl Cellulose on Copper

Mei-Ming Li, Qun-Jie Xu[*]*, Jie Han, Hong Yun, YuLin Min*

Shanghai Key Laboratory of Materials Protection and Advanced Materials in Electric Power, Shanghai University of Electric Power, Shanghai 200090, China
[*]E-mail: xuqunjie@shiep.edu.cn

Received: 11 July 2015 / *Accepted:* 2 September 2015 / *Published:* 30 September 2015

In this paper, Sodium carboxymethyl cellulose (Na-CMC), as a new green corrosion inhibitor, has been investigated. The inhibition behavior of Na-CMC on copper in simulated cooling water was examined by EIS and polarization measurements. The results showed that the best inhibition efficiency could reach to 83.34% when the concentration of Na-CMC is 5mg/L at 20^{o}C. The computing result of thermodynamic parameters (such as △G and △H) indicated that the adsorption of Na-CMC on the copper surface obeyed Langmuir's adsorption isotherm and was a typical of chemisorption. Quantum chemical calculations revealed that Na-CMC could be adsorbed on copper by Carboxyl group, which may be the suitable adsorption site, and its average adsorption energy was -60.823KJ/mol.

Keywords: organic coatings; copper; AFM; polarization; alkaline corrosion

1. INTRODUCTION

Copper and its alloys are extensively used in various industry applications owing to their excellent electrical and thermal conductivities, mechanical workability and corrosion resistance properties. However, in the presence of chlorides[1], sulphates[2] or bicarbonates[3] ions they are exposed to localized corrosion, which limits their practical application, especially in heating and cooling system.

Inhibitors are widely used for the corrosion protection of copper and its alloys. Most of the reported inhibitors are synthetic organic compounds containing heterocyclic atoms (nitrogen, sulfur, and phosphorous). Although these synthesized inhibitors, such as thiadiazole and its derivatives, have shown high corrosion inhibitive effect, they would pollute the environment during the process of their production and applications [4-5]. Therefore, it is significant to find environmentally friendly alternatives instead of the traditional corrosion inhibitors. Green corrosion inhibitors, such as

polyaspartic acid[6], amino acids[7], caffeic acid[8],etc, have aroused extensive attention. However, their applications were limited by two main defects. One is high cost and another is the high amount of green corrosion inhibitor.

Sodium carboxymethyl cellulose (Na-CMC), as a non-toxic, natural soluble modified cellulose, is widely used in food, pharmaceutical and other industries. Its molecular structure is shown in Figure 1. Compared with other green corrosion inhibitor, Na-CMC has advantages of abundant resources, natural biodegradability, less dosage and lower price[9-11] because it contains abundant hydroxyl groups . However, few papers have been reported about its corrosion inhibition of metals in solution. In this paper, the inhibition behavior of Na-CMC on copper in simulated cooling water would be investigated by EIS and polarization measurements. The thermodynamic parameters were calculated and discussed. In addition, the mechanism of adsorption was studied from the perspective of quantum chemistry.

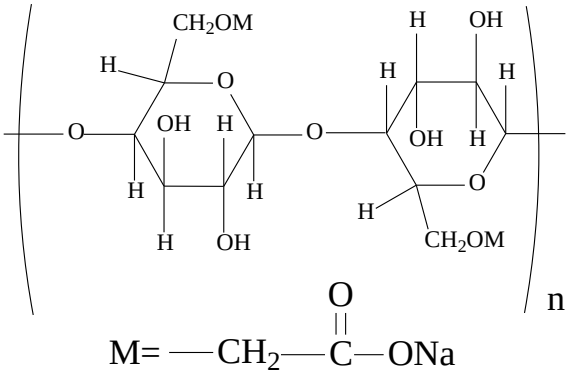

Figure 1. Molecular structure of Na-CMC

2.EXPERIMENTAL

2.1Materials and chemicals

Commercially pure copper (99.95 wt.%,) was used in this study. Sodium carboxymethyl cellulose（Na-CMC ,cp）was purchased from Sinopharm Chemical Reagent Co.,Ltd.

2.2 Instruments

Electrochemical studies were carried out using EG&G PARC Model 273 Potentiostat/

Galvanostat and PARC M1025 frequency response detector. For the measurement of EIS, the frequency range was 100 kHz - 0.05 Hz; the amplitude was 5 mV and the scan rate of Tafel curves was set between -0.25 and 0.25 V(vs OCP) at 1 mV/s. The morphologies of the samples were observed with a commercial Agilent 5500 AFM (Agilent Technologies ,USA). IR spectra were recorded with a FTIR-8400S Infrared Spectrometer (SHIMADZU of Japan).

2.3 Methods

Before each experiment, the working electrode was first mechanically polished with various grades of sandpaper (up to 1200 grit) and then ultrasonic cleaned in ethanol for 5 min, rinsed with deionized water, and then dried in air. A platinum sheet electrode was used for the counter electrode, and the reference electrode was a saturated calomel electrode (SCE).

The working electrodes (samples) were enveloped by epoxy resin and only remained an exposed area (0.785cm^2) for testing. All potentials were indicated against the SCE. Simulated cooling water ([NaCl] = 39mg / L, [Na_2SO4] = 90mg / L, [NaHCO3] = 70mg / L) was used as the corrosion medium. All experiments were performed at 20 ± 1℃.

2.4 Quantum chemical study

The electronic properties of Na-CMC was investigated at the level of B3LYP with 6-311++G (d,p) basis sets using the standard Gaussian 09 software package. The following quantum chemical indices were taken into consideration: the energy of the highest occupied molecular orbital (E_{HOMO}), the energy of the lowest unoccupied molecular orbital (E_{LUMO}), energy gap, $\triangle E = E_{HOMO}-E_{LUMO}$ and Mulliken charges and so on. Further, the adsorption energy on the Cu(110), Cu (111) and Cu (100) surfaces were conducted with DMol3 module in Materials Studio software.

3. RESULTS AND DISCUSSION

3.1 Electrochemical impedance spectroscopy

Fig. 2 presents EIS for mild steel electrode in simulated cooling water in the absence and presence of Na-CMC at various concentrations. Generally, the Nyquist plots are regarded as an arc. The impedance diagrams obtained are depressed into the x-axis and not perfect semicircles because of the known "the dispersing effect"[12-13] . With the increasing of concentration, the arc diameter gradually increased, and the corresponding impedance value also tended to increase, till the best inhibitor concentration reached to 5 mg / L. However, when the concentration increased to 8mg / L, the impedance value slightly reduced accordingly, known as the extreme phenomenon [14].

The impedance parameters were calculated by fitting the experimental results to an equivalent circuit using ZView software. In this model (Fig. 3), the R_s is solution resistance; the R_{ct} is charge transfer resistance, and the CPE is constant phase Element. The electrochemical parameters were presented in Table 1. The capacitance value was calculated by the following equation (1)[15]:

$$C_{dl} = (Y_O \cdot R_{ct}^{1-n})^{1/n} \quad (1)$$

Where C_{dl} is double layer capacitance, Y_0 is the magnitude of admittance of CPE; n is the exponential term and R_{ct} is the charge transfer resistance. Inhibition efficiency (IE%) was given by the following equation (2) [16]:

$$IE(\%) = \frac{R_{ct(inh)} - R_{ct(0)}}{R_{ct(inh)}} \times 100 \qquad (2)$$

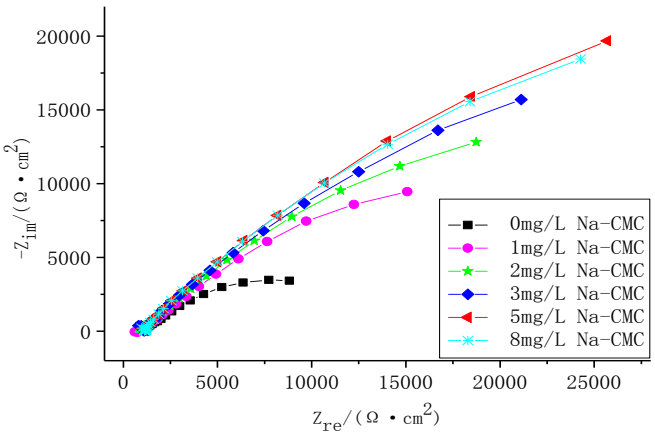

Figure 2. Nyquist plots of copper electrodes with different concentrations of Na-CMC.

Here $R_{ct(0)}$ and $R_{ct(inh)}$ are the uninhibited and inhibited charge transfer resistance, respectively. As can be seen from Table 1, the R_{ct} and IE% values would increase as the concentration of Na-CMC increased. It indicates that the water molecules are gradually replaced by the adsorption of inhibitor molecules at copper/solution interface to protect its surface from corrosion [17]. Therefore, the decrease in C_{dl} can be explained by the increase in the double layer thickness or the decrease in the local dielectric constant [18].

Table 1. AC impedance parameters of copper electrode with different concentrations of Na-CMC.

C/(mg/l)	$R_S/(\Omega \cdot cm^2)$	$Y_O/(\mu s \Omega cm^{-2})$	n	$C_{dl}/(\mu F \cdot cm^{-2})$	$R_{ct}/(\Omega \cdot cm^2)$	IE%	θ
0	1034	130.09	0.51	297.85	18205	/	/
1	1069	80.68	0.55	249.39	49677	63.35	0.6335
2	1027	64.89	0.58	180.23	61762	70.52	0.7052
3	1010	59.06	0.59	165.50	75137	75.77	0.7577
5	991.2	52.10	0.59	161.41	99610	81.72	0.8172
8	994.2	52.00	0.60	144.79	88024	79.32	0.7932

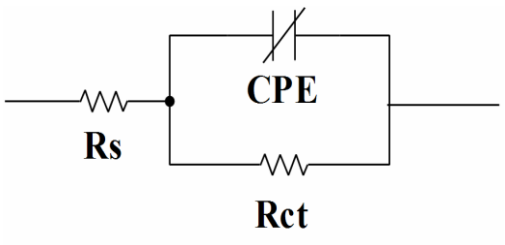

Figure 3. Equivalent circuit model for Nyquist plots

Bode plots for copper in simulated cooling water with and without inhibitor at different concentrations are shown in Fig. 4, which could confirm that the increase of absolute impedance at low frequencies in Bode plots shows the higher protection with increasing the concentration of Na-CMC. But when the concentration increased to 8mg / L, the impedance value slightly reduced, known as the extreme phenomenon [14], which agrees with the results of the Nyquist plot.

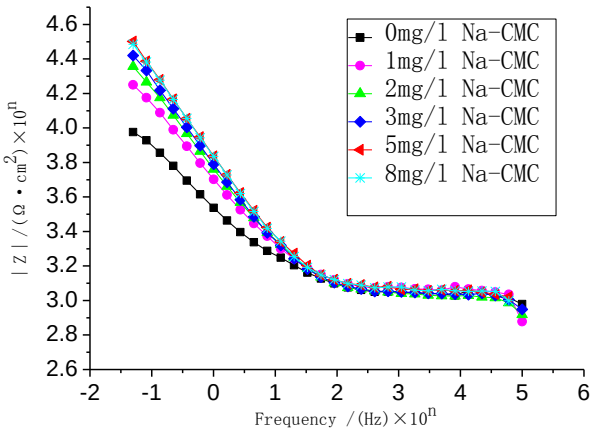

Figure 4. Nyquist plots of copper electrodes with different concentrations of Na-CMC.

3.2 Potentiodynamic polarization

Fig. 5 presents polarization curves for copper in simulated cooling water, in the absence and presence of Na-CMC at various concentrations. It is observed from the Tafel polarization curves (Fig.5) that both cathodic and anodic curves could show a lower current density in the presence of Na-CMC than those in the absence of Na-CMC. The anodic dissolution of copper and the cathodic reduction of oxygen are significantly inhibited. This suggests that Na-CMC is a mixed type (cathodic/anodic) of inhibitor [19]. The corrosion kinetic parameters namely the corrosion potential (E_{corr}), corrosion current density (I_{corr}), anodic Tafel slope (β_a) and cathodic Tafel slope (β_c) are summarized in Table2. The inhibition efficiency is defined as [20]:

$$IE(\%) = \frac{I_{coor(0)} - I_{coor(inh)}}{I_{coor(0)}} \times 100 \qquad (3)$$

Where $I_{corr(0)}$ and $I_{corr\ (inh)}$ are the corrosion current density without and with inhibitor, respectively. It can be observed that the concentration of Na-CMC has a little influence on the values of anodic Tafel slope (βa), but more significant influence on the values of cathodic Tafel slope (βc), indicating that the inhibitor may affect the mechanism of cathodic reaction and may not suppress the process of anodic dissolution[21]. In addition, the increase in inhibition efficiency is associated with a shift towards lower corrosion current densities and more positive E_{corr}, suggesting that Na-CMC acted as a mixed type of inhibitor to cathode. The results obtained from polarization curves showed good agreement with those obtained from EIS.

Table 2. Polarization curve parameters of copper electrode with different concentrations of Na-CMC.

C (mg/l)	β_a ($mvdec^{-1}$)	β_c ($mvdec^{-1}$)	E_{coor} (mv)	I_{coor} (μAcm^{-2})	IE%	θ
0	136.05	388.51	-50.24	3.008	/	0
1	103.24	212.27	-56.48	1.138	62.17	0.6217
2	101.10	207.54	-55.31	1.067	64.53	0.6453
3	97.82	195.56	-45.64	0.820	72.73	0.7273
5	93.34	185.52	-42.66	0.681	77.35	0.7735
8	91.66	194.86	-41.12	0.730	75.73	0.7573

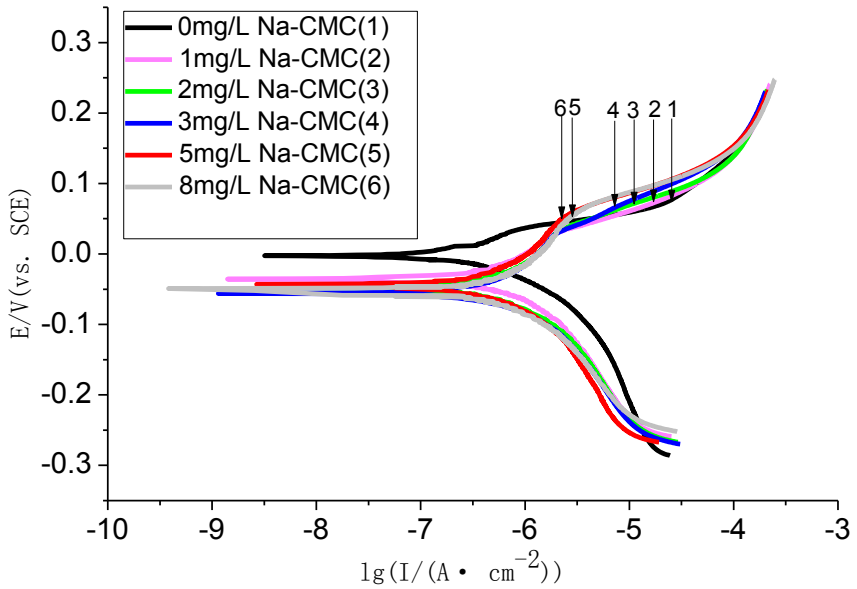

Figure 5. Tafel plots of copper electrodes with different concentrations of Na-CMC.

3.3 AFM

The AFM images (3.5μm×3.5μm) and (1μm×1μm) of copper polished after immersed in simulated water with and without 5mg/L Na-CMC at 303.15k for 12h were given in Fig.6. It can be seen that significant differences after addition of Na-CMC are found on the surface morphology of the corroded specimen. The surface morphology of copper immersed in simulated water with 5mg/LNa-CMC is more uniform than the surface in the absence of Na-CMC, similar with the surface morphology of copper polished. The average roughness (sq) of different specimens was listed in table 3. The average roughness of the copper surface in inhibited solution was 3.89nm(1μm×1μm), which was similar with the roughness of copper surface polished, while the average roughness of the copper immersed in simulated water without 5mg/L was 12.7 nm(1μm×1μm). The AFM images indicated that the Na-CMC could be adsorbed on the copper surface and then would reduce the corrosion rate of the copper.

Table 3. The average roughness of copper polished, immersed in simulated water with and without 5mg/L Na-CMC.

The scan area	polished copper(sq)/nm	copper immersed in simulated water with 5mg/L Na-CMC (sq)/nm	copper immersed in simulated water without 5mg/L Na-CMC (sq)/nm
1μm×1μm	3.02	3.89	12.7
3.8μm×3.8μm	6.41	5.52	18.1

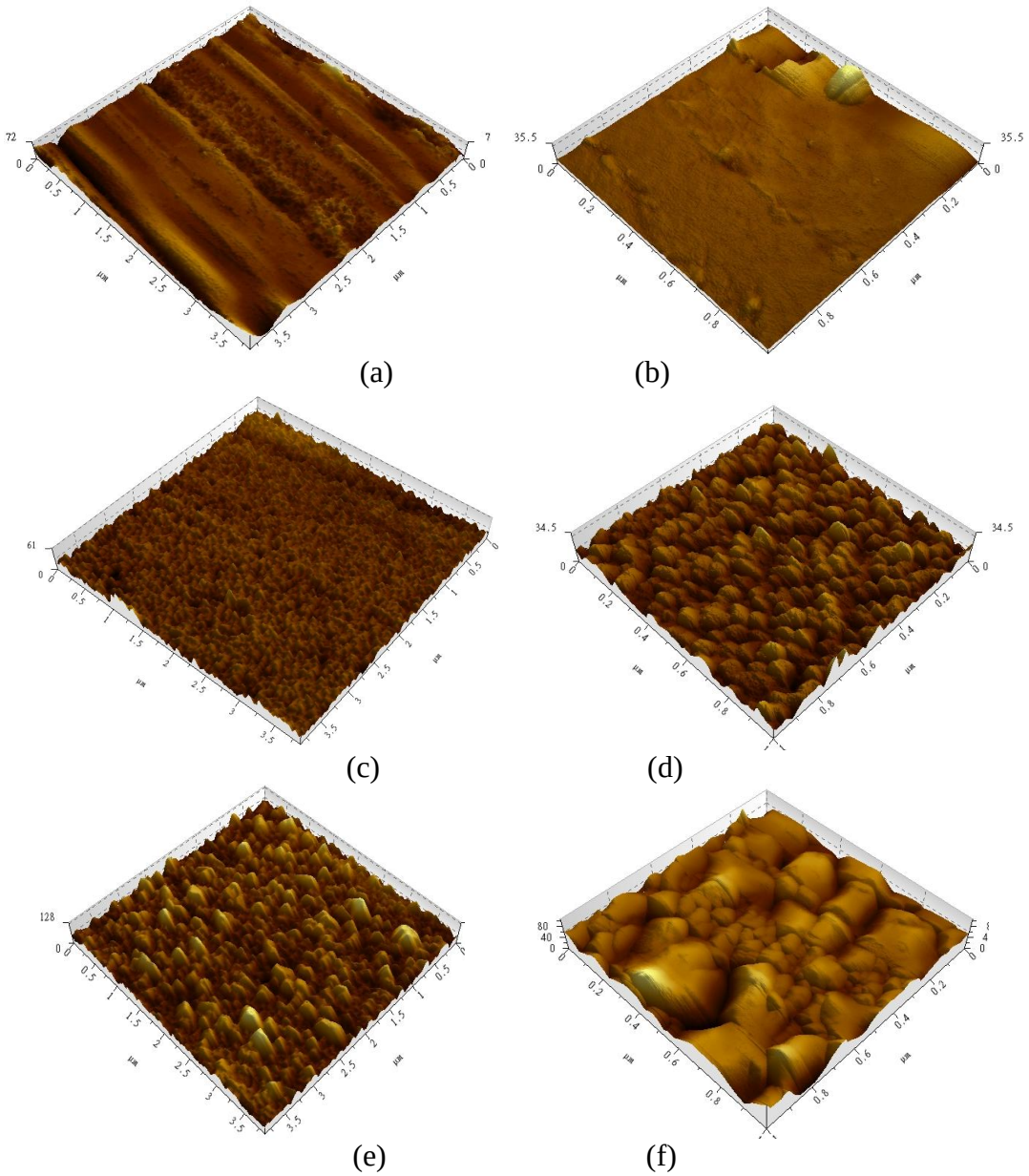

Figure 6. AFM images of copper (a)polished copper (3.5μm×3.5μm), (b)polished copper (1μm×1μm),(c)Inhibited copper (3.5μm×3.5μm),(d) Inhibited copper (1μm×1μm),(e)copper in simulated water (3.5μm×3.5μm),(f) copper in simulated water(1μm×1μm).

3.4 FT-IR

The FT-IR spectra of Na-CMC powder and the layer formed on the copper specimen immersed in simulated cooling water containing Na-CMC of 5mg/L are shown in Fig. 7. For pure Na-CMC powder (Fig7.a), the peaks in the region of 3422, 2923, 1623, 1417 cm^{-1} correspond to the O-H, C-H, COO^-(asymmetric), COO^- (symmetric) stretching vibration [22-23] respectively. However, compared with Na-CMC powder removed from the surface of copper (Fig.7b), there is a band shifted in the region of 1583 and1388 cm^{-1}. These results indicate that the adsorption of Na-CMC may occur between the copper and the free COO^- group in the ring of Na-CMC. On the other hand, Na-CMC could be adsorbed on copper by carboxyl group, which may be the suitable adsorption site.

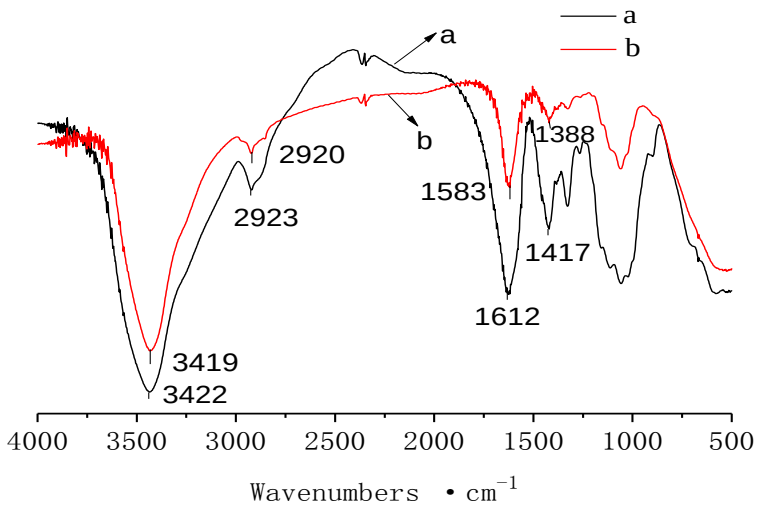

Figure 7. FT-IR spectra of Na-CMC

3.5 Adsorption isotherm

To understand the mechanism of corrosion inhibition, it is necessary to examine the adsorption behavior of Na-CMC on the copper surface. The isotherms describing the adsorption behavior of corrosion inhibitor is essentially established because they could provide important information about the nature of metal–inhibitor interaction. The degree of surface coverage (θ) calculated for different concentrations of Na-CMC were tested graphically by fitting to various adsorption isotherms including Frumkin, Temkin, Langmuir and Freundlich isotherms[24]. The best fit was obtained from the Langmuir isotherm, which can be given by the following equation[25-26]:

$$\frac{C}{\theta} = \frac{1}{K_{ads}} + C \qquad (4)$$

Where C is inhibitor concentration, θ is the degree of the coverage on the copper surface(listed in the table2), K_{ads} is the adsorption–desorption equilibrium constant.

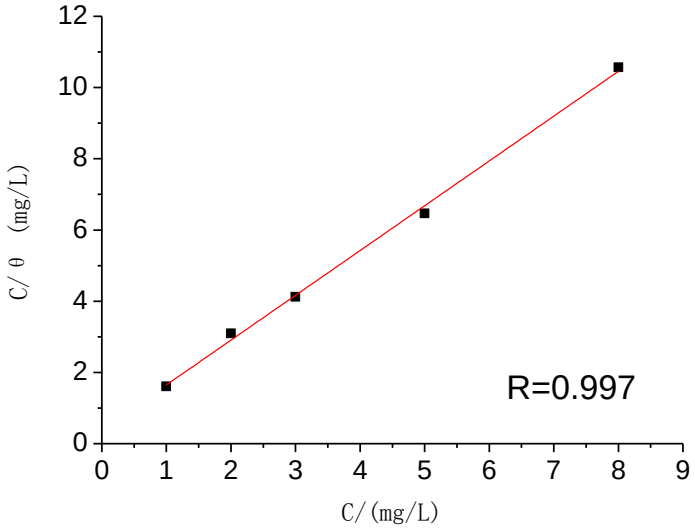

Figure 8. Langmuir isotherm model of Na-CMC on copper

Fig. 8 shows the plots of C/θ versus C and the correlation coefficient is higher than 0.99, which suggests that the experimental data are well conformed to Langmuir isotherm. Equation (4) can be written as:

$$\frac{C}{\theta} = 0.393 + 1.258C$$

The K_{ads} is $K_{ads}=2.544\times10^3$L/g, corresponding to 5.572×10^5 L/mol, which reflects the high adsorption ability of Na-CMC on the copper surface. Further, it is related with the standard free energy of adsorption $\triangle G_{ads}$ according to the following equation [25-26]:

$$K_{ads} = \frac{1}{55.5}\exp(^{-\Delta G_{ads}}/_{RT}) \quad (5)$$

Where R and T are the gas constant and the thermodynamic temperature respectively, the calculated $\triangle G_{ads}$ is -42.040KJ/mol. The calculated values of $\triangle G_{ads}$ indicate that the adsorption mechanism of Na-CMC on copper surface in simulated cooling water is chemisorption [27].

3.6 Effect of temperature

Polarization measurements were performed at different temperatures (from 293K to 323 K) in the absence and presence of Na-CMC of 5mg/L to prove the activation energy of dissolution of copper. The activation energy of the corrosion process was calculated by the Arrhenius equation（ 6）[28]:

$$I_{coor} = A\exp(^{-E_a}/_{RT}) \quad (6)$$

Where E_a is the activation energy, I_{corr} is corrosion current, R the gas constant and T the thermodynamic temperature respectively. When plotting $\ln I_{corr}$ versus $10^3\times1/T$, the values of E_a can be calculated by the slopes of straight lines (Fig. 9). The Ea determined from the slope of the Arrhenius plots corresponds to 13.104 kJ/mol in the absence and 39.488 kJ/mol in the presence of Na-CMC,

respectively. The higher value of activation energy in the presence of Na-CMC indicates the higher protection efficiency of the inhibitor [29].

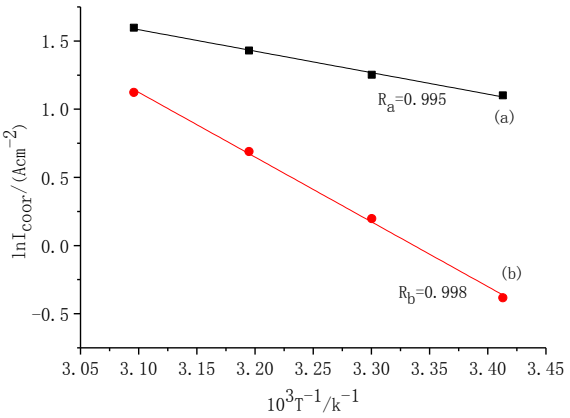

Figure 9. lnIcoor vs 103×1/T curves of copper electrodes without (a) and with (b) 5mg/L Na-CMC

ΔH_{ads} of Na-CMC on copper surface was related with the Langmuir adsorption isotherm and was calculated from following equation (7) [30]:

$$\ln\left(\frac{\theta}{1-\theta}\right) = \ln A + \ln C - \frac{\Delta H_{ads}}{R}\frac{1}{T} \qquad (7)$$

Where θ is the degree of the coverage (listed in table4), A the independent constant, C the inhibitor concentration, R the gas constant, ΔH_{ads} the heat of adsorption, and T is the thermodynamic temperature. A plot of ln(θ/(1-θ)) versus $10^3$1/T is given in Fig10. The slope of the linear parts of the curve is equal to ΔH_{ads}, from which the heat of adsorption ΔH_{ads} was calculated as -44.925 KJ/mol. The negative value of the standard heat of the adsorption process indicates that the adsorption process is exothermic in nature. The entropy (ΔS_{ads}) of adsorption can be calculated by the following equation （8）[31]:

$$\Delta G_{ads} = \Delta H_{ads} - T\Delta S_{ads} \qquad （8）$$

The value of ΔS_{ads} is calculated as -8.852 $Jmol^{-1}K^{-1}$, which indicates that copper surface becomes more orderly after corrosion with the formation of the inhibitor molecules film [14].

Table 4. Electrochemical parameters of copper electrodes without and with 5mg/L Na-CMC

T/K	$I_{corr\ (0)}$ (μAcm^{-2})	$I_{corr\ (inh)}$ (μAcm^{-2})	IE%	θ
293	3.008	0.6814	77.35	0.7735
303	3.479	1.219	65.14	0.6514
313	4.178	1.991	52.34	0.5234
323	4.942	3.075	37.78	0.3778

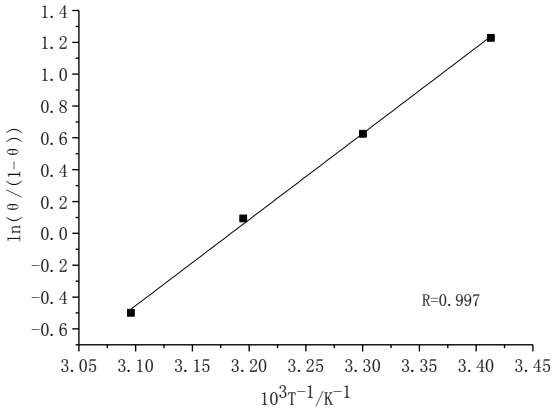

Figure 10. ln(θ/(1-θ)) vs 103×1/T curves of copper electrodes with 5 mg/L Na-CMC.

3.7 Quantum chemical calculations

To investigate the effect of molecular structure on inhibition efficiency and the inhibition mechanism, some quantum calculations are performed. The geometries of Na-CMC were fully optimized by the Gaussian 09 software package employing the B3LYP/6-311++G (d,p) method .

The charge distribution of molecule and the frontier molecule orbital density distributions of the molecules are given in Fig11a, b and c, respectively. The quantum chemical parameters of Na-CMC was listed in table5. It has been reported that the higher HOMO energy of the inhibitor, the greater trend of donating electrons to the metal; the lower LUMO energy, the easier acceptance of electrons from metal surface; lower values of the energy of the gap △E will render better inhibition efficiencies[32-33]. The lowest unoccupied molecular orbital (LUMO) is located on the carboxyl functional group, and the Mulliken charge of oxygen atoms on the carboxyl functional group are -0.473 and -0.451, respectively ,which is larger than others.

Table 5. quantum chemical parameters of Na-CMC

E_{HOMO} eV	E_{LUMO} eV	ΔE eV	μ Debye	Total Energy eV
-1.3627	0.7674	2.1301	25.4853	-24892.4

Therefore, it can be believed that Na-CMC could be adsorbed on copper by carboxyl group, which may be the suitable adsorption site. The results obtained from quantum chemical calculations show good agreement with those obtained from FT-IR.

Molecular simulation study was performed employing DMol3 module to simulate the adsorption structure of the Na-CMC for understanding the interactions between Na-CMC and copper surface. The lowest layer of copper atoms was kept immobile while the upper two layers were allowed to relax during the entire simulation. The exchange–correlation functional employed was the

generalized gradient approximation method, known as GGA-PBE. A 2×2×1 k-point sampling was used for all the slabs. The surfaces of Cu(100), Cu (110) and Cu (111), the molecule Na-CMC and the adsorption modeling of Na-CMC on the copper surfaces were shown in Fig. 12,a,b,c,d,e,f,g,h and i after the geometry optimization, respectively.

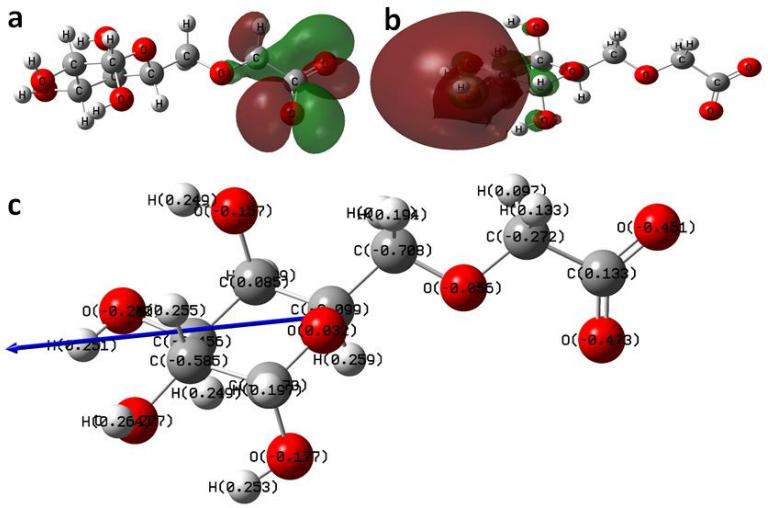

Figure 11. (a)The frontier molecular orbital (HOMO) of Na-CMC; (b)The frontier molecular orbital (LUMO) of Na-CMC; (c)Charge distribution of Na-CMC

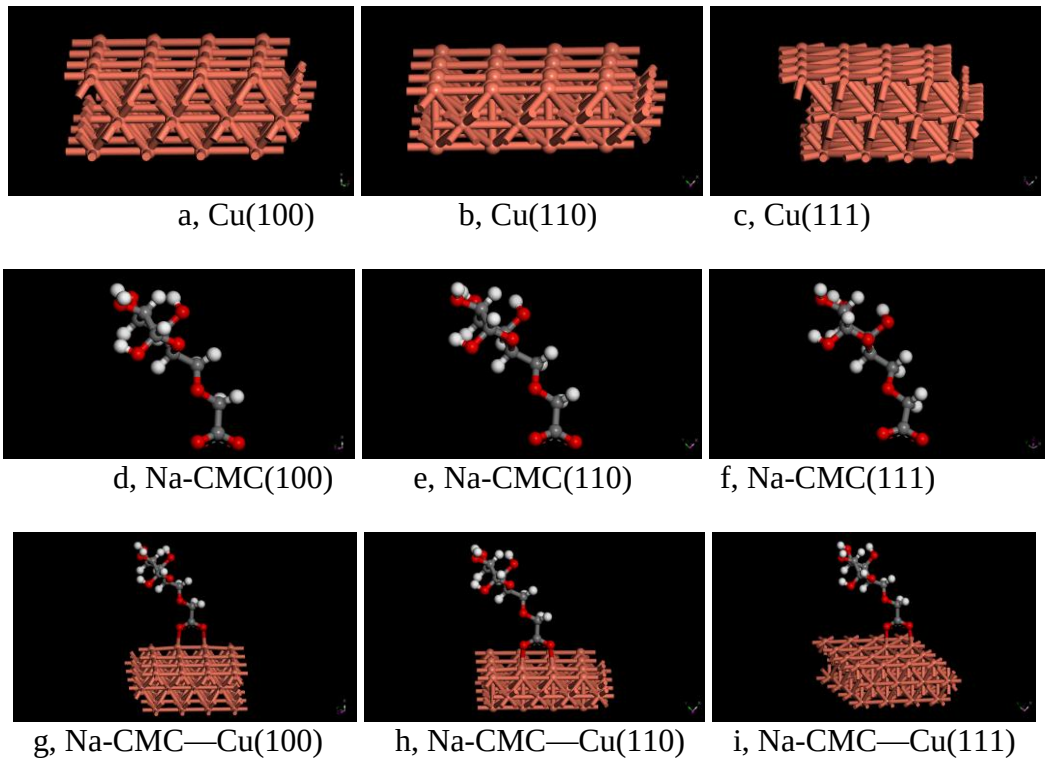

a, Cu(100) b, Cu(110) c, Cu(111)

d, Na-CMC(100) e, Na-CMC(110) f, Na-CMC(111)

g, Na-CMC—Cu(100) h, Na-CMC—Cu(110) i, Na-CMC—Cu(111)

Figure 12. The surfaces of Cu(100), Cu (110) and Cu (111) ,the molecule Na-CMC and the adsorption modeling of Na-CMC on the copper surfaces ,were shown in Fig. 12,a,b,c,d,e,f,g,h,i, after the geometry optimization ,respectively.

Table 6. The adsorption energies of Na-CMC

The plane of Cu	$E_{molecular}$ (Ha)	$E_{surface}$ (Ha)	E_{total} (Ha)	$E_{adsorption}$ (Ha)	$E_{adsorption}$ (KJ/mol)
Cu(100)	-913.882	-10681.3	-11595.2	-0.02864	-75.2048
Cu(110)	-913.887	-10680.9	-11594.9	-0.02561	-67.2391
Cu(111)	-913.877	-10681.4	-11595.3	-0.01524	-40.0247

The calculated electronic energies of the Na-CMC molecule($E_{molecule}$), the copper surface ($E_{surface}$), and the total energy(E_{tot}) of the metal are listed in the table 6. The adsorption energy of Na-CMC on copper was calculated by equation(9):

$E_{adsorption}=E_{total}-E_{molecule}-E_{surface}$[25] (9)

It can be seen that the adsorption energy of Cu(100), Cu (110) and Cu (111) were -75.2048, -75.2048 and -40.0247, respectively, which showed that the adsorption of Na-CMC on Cu(100) was the most reliable. Its average adsorption energy was -60.823KJ/mol, which indicated the strong chemisorption of Na-CMC on copper surface.

4. CONCLUSIONS

As a new type of green corrosion inhibitor, sodium carboxymethyl cellulose (Na-CMC) has some advantages of easy biodegradability, low price and small consumption, etc. According to the results from electrochemical polarization and EIS measurements and FT-IR, the conclusions of this study can be summarized as following:

(1)The best inhibition efficiency of Na-CMC was 81.72% when its concentration reached 5mg/L at 20^{o}C;

(2) The computing result of thermodynamic parameters (such as ΔG and ΔH) indicated that the adsorption of Na-CMC on the copper surface obeyed Langmuir's adsorption isotherm and was a typical of chemisorption;

(3) The calculations of quantum chemistry revealed that Na-CMC could be adsorbed on copper by carboxyl group which may be the suitable site for adsorption and its average adsorption energy was -60.823KJ/mol.

ACKNOWLEDGEMENTS

This work was financially supported by Key Project of Shanghai Education Committee (No. 14ZZ152) and Shanghai Science and Technology Committee (No. 14DZ2261000).

References

1. H.W. Tian,W.H. Li, B.Hou, *Int.J.Electrochem.Sci.*, 8 (2013) 8513.

2. B.A.Abd-El-Nabey,A.M.Abdel-Gaber,E.Khamis,Aly.I.A.Morgaan and N.M.Ali , *Int.J.Electrochem.Sci.*, 8 (2013) 11301-11326.
3. R.Bostan. S.Varvara, L. Găină, L.M. MureŞan, *Corros.Sci.*, 63 (2012) 275.
4. Y. Huang, D.K. Sarkar, D. Gallant, X.G. Chen, *Appl. Surf. Sci.*, 282 (2013) 689-694.
5. M. Antonijević, S. Milić, M. Petrović, *Corros.Sci.*, 51 (2009) 1228.
6. B.R Zhang, C. J. He, C Wang, Y Lin, *Corros. Sci.*, 94 (2015) 6-20.
7. M. Bobina, A. Kellenberger, J. Millet, C. Muntean, N. Vaszilcsin, *Corrosion.Sci.*, 69 (2013) 389.
8. Y.H. Gao, L.H Fan, L.Ward, Z. F Liu, *Desalination*, 365 (2015) 220–226.
9. D. Gelmana, D. Starosvetskyb, Y. Ein-Elia, *Corros. Sci.*, 82 (2014) 271-279.
10. H. X. Qiu, J. G.Yu, T. Lin, *Acta Polymerica Sinica*, 3 (2004) 419.
11. M.M. Solomon , S.A. Umoren , I.I. Udosoro, A.P. Udoh, *Corros.Sci.*, 52 (2010) 1317.
12. Z. Wang, J. Gong, J. Ma, J. Xu, RSC. *Adv.* 4 (2014) 14708-14714.
13. P. Wang, D. Zhang, R. Qiu, Y. Wana, J. Wu, *Corros. Sci.*, 80 (2014) 366-373.
14. Q. J. Xu, L.J. Zhu , W.M. Cao, Z.Y.Wan, G.D. Zhou, Ch. J. Lin, *Acta Phys. -Chim. Sin.*, 24 (2008) 1724.
15. M. Mahdavian, S. Ashhari, *Electrochimica Acta* ,55 (2010) 1720.
16. G. Quartarone, M. Battilana, L. Bonaldo, T. Tortato, *Corros.Sci.*, 50 (2008) 3467.
17. H. Tian, W. Li, B. Hou, *Corros.Sci.*, 53 (2011) 3435.
18. L.Ch. Hu, Sh.T. Zhang, W.H. Li, B. Hou, *Corros.Sci.*, 52 (2010) 2891.
19. Q.Y. Liu, L.J. Mao, S.W. Zhou, *Corros. Sci*. 84 (2014) 165–171.
20. D. Gopi, K. M. Govindaraju, V. Collins Arun Prakash, D.M. Angeline Sakila, L. Kavitha, *Corros.Sci.*,51 (2009) 2259.
21. H. Gerengi, H.I. Sahin, *Industrial & Engineering Chemistry Research* , 51 (2012) 785.
22. A.H. Hebeish, M. Hashem, M.M. Abd El-Hady, S. Sharaf, *Carbohydrate Polymers*,92 (2013) 407.
23. A. I. Raafat, M. Eid, M. B. El-Arnaouty, *Nuclear Instruments and Methods in Physics Research B*, 283 (2012) 71.
24. A.k.Singh, S.K.Shukla, M.A. Quraishi, E.E.Ebenso, *Journal of the Taiwan Institute of Chemical Engineers*, 43 (2012) 463.
25. S. S. Abd ElRehim, S.M. Sayyah, M. M. El-Deeb, S. M. Kamal, R. E. Azooz, *Materials Chemistry and Physics*, 123 (2010) 20.
26. Y.Zhou,Sh.T.Zhang,L.Guo,Sh.Y.Xu,H.Lu,F.Gao,*Int.J.Electrochem.Sci.*,10 (2015) 2072-2087.
27. C. M. Goulart, A. Esteves-Souza, C. A. Martinez-Huitle, C. J. F. Rodrigues, M. A. M. Maciel, A.Echevarria, *Corros.Sci.*, 67 (2013) 281.
28. A. K. Satpati, P.V.Ravindran, *Materials Chemistry and Physics*, 109 (2008) 352.
29. F.F. Eliyan, A. Alfantazi, *Corros. Sci*., 85 (2014) 380–393
30. A. Döner, G. Kardaş, *Corros.Sci.*,53 (2011) 4223.
31. M. A. Hegazy, M. Abdallah, H. Ahmed, *Corros.Sci.*,52 (2010) 2897.
32. M. Behpour, S. M. Ghoreishi, M. Khayatkashani, M. Soltani , *Corros.Sci.*, 53 (2011) 2489.
33. N. Soltani, N. Tavakkoli, M. Khayatkashani, M. Reza.Jalali, A. Mosavizade, *Corros. Sci.*, 62 (2012) 122.